Y3.N88:25/4891

NUREG/CR-4891
PNL-6164

ORIGINAL

Properties of Reactor Fuel Rod Materials at High Temperatures

Final Summary Report
Severe Core Damage Property Tests Program

Prepared by J. T. Prater, E. L. Courtright

Pacific Northwest Laboratory
Operated by
Battelle Memorial Institute

Prepared for
U.S. Nuclear Regulatory Commission

BEST COPY AVAILABLE

COMPLETED

NOTICE

This report was prepared as an account of work sponsored by an agency of the United States Government. Neither the United States Government nor any agency thereof, or any of their employees, makes any warranty, expressed or implied, or assumes any legal liability of responsibility for any third party's use, or the results of such use, of any information, apparatus, product or process disclosed in this report, or represents that its use by such third party would not infringe privately owned rights.

NOTICE

Availability of Reference Materials Cited in NRC Publications

Most documents cited in NRC publications will be available from one of the following sources:

1. The NRC Public Document Room, 1717 H Street, N.W. Washington, DC 20555
2. The Superintendent of Documents, U.S. Government Printing Office, Post Office Box 37082, Washington, DC 20013-7082
3. The National Technical Information Service, Springfield, VA 22161

Although the listing that follows represents the majority of documents cited in NRC publications it is not intended to be exhaustive.

Referenced documents available for inspection and copying for a fee from the NRC Public Document Room include NRC correspondence and internal NRC memoranda; NRC Office of Inspection and Enforcement bulletins, circulars, information notices, inspection and investigation notices; Licensee Event Reports; vendor reports and correspondence; Commission papers; and applicant and licensee documents and correspondence.

The following documents in the NUREG series are available for purchase from the GPO Sales Program: formal NRC staff and contractor reports, NRC-sponsored conference proceedings, and NRC booklets and brochures. Also available are Regulatory Guides, NRC regulations in the *Code of Federal Regulations*, and *Nuclear Regulatory Commission Issuances*.

Documents available from the National Technical Information Service include NUREG-series reports and technical reports prepared by other federal agencies and reports prepared by the Atomic Energy Commission, forerunner agency to the Nuclear Regulatory Commission.

Documents available from public and special technical libraries include all open literature items, such as books, journal and periodical articles, and transactions. *Federal Register* notices, federal and state legislation, and congressional reports can usually be obtained from these libraries.

Documents such as theses, dissertations, foreign reports and translations, and non-NRC conference proceedings are available for purchase from the organization sponsoring the publication cited.

Single copies of NRC draft reports are available free, to the extent of supply, upon written request to the Division of Information Support Services, Distribution Section, U.S. Nuclear Regulatory Commission, Washington, DC 20555.

Copies of industry codes and standards used in a substantive manner in the NRC regulatory process are maintained at the NRC Library, 7920 Norfolk Avenue, Bethesda, Maryland, and are available there for reference use by the public. Codes and standards are usually copyrighted and may be purchased from the originating organization or, if they are American National Standards, from the American National Standards Institute, 1430 Broadway, New York, NY 10018.

BEST COPY AVAILABLE

NUREG/CR-4891
PNL-6164

Properties of Reactor Fuel Rod Materials at High Temperatures

Final Summary Report
Severe Core Damage Property Tests Program

Manuscript Completed: May 1987
Date Published: July 1987

Prepared by
J. T. Prater, E. L. Courtright

Pacific Northwest Laboratory
Richland, WA 99352

Prepared for
Division of Reactor Accident Analysis
Office of Nuclear Regulatory Research
U.S. Nuclear Regulatory Commission
Washington, DC 20555
NRC FIN B2455

ABSTRACT

This report summarizes work sponsored by the U.S. Nuclear Regulatory Commission Division of Accident Evaluation to investigate those physical properties that are needed to predict the behavior of fuel-rod assemblies during a loss-of-coolant accident. The results include a determination of the oxidation kinetics of Zircaloy and Zircaloy-uranium oxide mixtures in steam and steam-hydrogen gas mixtures at 1300 to 2400°C, viscosity measurements on zirconium-uranium oxide mixtures at 1800 to 2100°C, an estimate of the heat of reaction for the dissolution of uranium oxide by molten zirconium at 2000°C, and thermal diffusivity measurements on prereacted Zircaloy-uranium oxide mixtures at 800 to 1500°C.

BLANK PAGE

SUMMARY

The high temperature properties of Zircaloy and zirconium-uranium oxide mixtures have been measured to assist the Nuclear Regulatory Commission in assessing the behavior of fuel-rod assemblies during a loss-of-coolant accident. Specific properties studied included the oxidation behavior of Zircaloy and Zircaloy-UO_2 mixtures in steam and steam-hydrogen atmospheres, the viscosity of molten zirconium-UO_2 mixtures, the heat of reaction for dissolution of UO_2 in molten zirconium, and the thermal diffusivity of prereacted Zircaloy-UO_2 mixtures.

Isothermal oxidation kinetics of Zircaloy-4 have been measured from 1300 to 2400°C in steam and steam hydrogen atmospheres. Growth kinetics in the oxide layer were parabolic. The study confirmed a previous finding that a discontinuity exists in the oxide growth rate above 1500°C which coincides with the tetragonal-to-cubic phase transformation in substoichiometric ZrO_2. Above 1500°C, the rates were found to lie slightly above those previously established by the Baker-Just relationship. No additional discontinuity in the oxide growth rate was observed when the metal phase melted.

The oxidation kinetics were found to be independent of steam pressure, flow rate, and hydrogen content, as long as sufficient steam was available to satisfy the requirements of the oxidation reaction. Oxidation experiments conducted in steam-hydrogen mixtures at 1565 and 1815°C revealed that concentrations of hydrogen up to 90 mol% had no effect on the oxidation kinetics. The rate controlling factor appeared to be diffusion through the oxide layer.

The oxidation kinetics of Zircaloy prereacted with 15 mol% UO_2 were also measured from 1400 to 2100°C. Growth rates comparable to those observed for Zircaloy above 1500°C were observed.

The viscosities of Zr-UO_2 mixtures with 0 to 30 mol% UO_2 were measured at temperatures to 2100°C. The viscosities of the molten liquids were nearly independent of UO_2 content and were bracketed between 10 and 17 centipoise. The apparent melting temperature where fluid behavior first appeared varied with composition. For Zr-UO_2 mixtures with greater than 15 mol% UO_2, fluid behavior appeared at a lower temperature upon initial heating than on subsequent cycles. This suggested that the apparent melting temperature was dependent on the microstructure of the solid UO_2 phase.

The heat of reaction for the dissolution of UO_2 in molten zirconium was measured at 2000°C. Experimental difficulties were encountered; however, a value of 20 kcal/mol of UO_2 was determined to be a reasonable estimate. In addition, thermal diffusivities of approximately 3 mm^2/s were measured between 800 and 1500°C on prereacted Zircaloy-UO_2 mixtures containing 15 and 30 mol% UO_2.

BLANK PAGE

ACKNOWLEDGMENTS

The authors are indebted to J. E. Garnier for designing and assembling the oxidation test apparatus; L. R. Bunnell, D. I. Boget and W. C. Morgan for performing the viscosity measurements; C. W. Griffin and J. L. Brimhall for conducting the thermal diffusivity and heat of reaction studies; M. L. Picklesimer for his technical advice; and R. Van Houten, the NRC program manager, for his advice and encouragement.

CONTENTS

ABSTRACT iii

SUMMARY v

ACKNOWLEDGMENTS vii

INTRODUCTION 1

EXPERIMENTAL PROCEDURE 3

OXIDATION KINETICS 3

VISCOSITY MEASUREMENTS 3

HEAT OF REACTION MEASUREMENTS 6

THERMAL DIFFUSIVITY MEASUREMENTS 7

RESULTS AND DISCUSSION 8

OXIDATION KINETICS 8

Isothermal Oxidation Kinetics 8

Effect of Temperature Gradients 11

Application to Transient Oxidation 14

Oxidation of Zircaloy-Uranium Oxide Mixtures 15

Effect of Steam Dilution by Hydrogen 18

VISCOSITY OF ZIRCONIUM-URANIUM OXIDE MIXTURES 21

HEAT OF REACTION FOR DISSOLUTION OF URANIUM OXIDE BY MOLTEN ZIRCONIUM 25

THERMAL DIFFUSIVITY OF ZIRCALOY-URANIUM OXIDE MIXTURES 26

SUMMARY 28

REFERENCES 29

FIGURES

1	Apparatus Used to Measure High-Temperature Oxidation of Zircaloy	4
2	Oscillating-Cup Viscometer	5
3	Schematic of the Apparatus Used to Measure the Heat of Reaction Between Zirconium and Uranium Oxide	6
4	Parabolic Rate Constants for Oxide Layer Growth	9
5	Micrograph of Zircaloy-4 Oxidized in Steam for 40 s at 1595°C	10
6	Zirconium-Oxygen Phase Diagram	12
7	Comparison of Parabolic Rate Constants for Oxide Layer Growth	13
8	Micrograph of a Zircaloy-15 mol% Uranium Oxide Sample Oxidized in Steam for 27 s at 1820°C Showing Preferential Oxidation of the Uranium-Rich Phase	16
9	Isothermal Parabolic Rate Constant for Oxide Layer Growth on Zirconium-15 mol% Uranium Oxide	17
10	Effect of Hydrogen on Oxidation Kinetics	19
11	Calculated Viscosity Values for Zircaloy-2 and Various Zirconium-Uranium Oxide Mixtures as a Function of Composition	22
12	Schematic Diagram of Flow Behavior as a Function of Temperature and Uranium Oxide Content	23
13	Micrograph of a Zr-30 mol% Uranium Oxide Sample After Heating to 2100°C	24
14	Thermal Analysis Curve for Zirconium-25 wt% Uranium Oxide	26
15	Thermal Diffusivity Measurements for Prereacted Zircaloy-Uranium Oxide Mixtures	27

TABLES

1 Comparison of Computed and Measured Layer Thicknesses Formed During Transient Oxidation 14

2 Hydrogen Analysis for Oxidized Zircaloy-4 Samples Using the Inert-Gas Fusion Technique 20

INTRODUCTION

The results of a research program investigating the material properties that are relevant to predicting the behavior of fuel-rod assemblies during a small-break loss-of-coolant accident (LOCA) are reported. These studies have been conducted under the Severe Core Damage Material Property Test Program. The objective of the program is to assist the U.S. Nuclear Regulatory Commission (NRC) in evaluating the damage that a nuclear reactor core and fuel assemblies might sustain during a LOCA. The experimental work was performed by Pacific Northwest Laboratory (PNL) for the NRC Division of Accident Evaluation. Specific properties studied include: 1) the oxidation behavior of Zircaloy-4 and Zircaloy-uranium oxide mixtures in pure steam and steam-hydrogen gas mixtures, 2) the viscosity and thermal diffusivity of molten zirconium-UO_2 mixtures, and 3) the heat of dissolution of UO_2 by zirconium.

When a small break occurs in the coolant system of a pressurized water reactor, severe core damage can result, as occurred at Three Mile Island-2 (TMI-2). In this type of accident, the top portion of the reactor may uncover. However, a reservoir of water may remain in the lower portion of the reactor to produce steam that allows cladding oxidation to continue. While loss of the moderator automatically shuts down the nuclear reaction, fission-product-decay heat in the fuel, combined with the heat released by the highly exothermic oxidation of the Zircaloy cladding, can drive fuel rod temperatures in the uncovered section of the fuel assemblies well above the melting point of Zircaloy. As the remaining unoxidized cladding melts, it may carry large amounts of dissolved fuel with it to the lower portions of the core. The redistribution of fuel into potentially noncoolable geometries and the generation of large volumes of hydrogen during cladding oxidation have serious consequences on reactor safety.

Since experimental data on the behavior of a full-sized reactor core under these conditions does not exist, the NRC is developing computer codes to provide best-estimate calculations of the core behavior. Small-scale in-reactor tests are being conducted to provide partial verification of these codes. The success of these computer codes depends on the incorporation of good materials property data. The high-temperature oxidation kinetics of Zircaloy is among the most critical because it is required to calculate the rate of energy release and the extent of cladding oxidation and hydrogen generation during the accident transient.

Current U.S. power plant licensing criteria established in 10 CFR 50 (U.S. Code of Federal Regulations 1981) require the use of the Baker-Just (1962) isothermal oxidation kinetics rates in all computer codes used to characterize cladding oxidation behavior during the transient. The Baker-Just rates were originally adopted because they would provide a conservative estimate of oxidation-induced cladding embrittlement during a large-break LOCA. In a large-break accident, (believed at the time to be the worst-case scenario for

nuclear reactor core accidents) the reactor core was rapidly emptied of all coolant. Because the temperature escalation was only driven by fission-product-decay heat, the reactor core temperature peaked at about 1300°C. The single major safety concern in the large-break LOCA was the shattering of the fuel rods during cooldown. Below 1500°C, the Baker-Just rates overestimated cladding oxidation, and thus, the extent of cladding embrittlement. These rates were used to establish criteria that avoid fuel fragmentation during core reflood.

In a small-break LOCA, the additional heat generated by the oxidation of the fuel cladding drives the thermal excursion to much higher temperatures. No single safety concern dominates under these conditions. In this case, the oxidation rates establish not only the extent of cladding oxidation and embrittlement but also the quantity of hydrogen generated and the rate of cladding-temperature escalation. It is also important for establishing the amount of unoxidized cladding that is present which can potentially melt, react with the fuel, and flow to the lower portions of the core. The complexity of the safety analysis makes it extremely important to establish realistic oxidation rates and to understand the limitations on the accuracy and use of the oxidation data.

The melting of the unoxidized cladding and the massive redistribution of the cladding and fuel to the lower portions of the core (into potentially non-coolable geometries) is also an extremely important consideration in the small-break LOCA. While some data exists on the properties of molten Zircaloy, nothing is known about the effect of dissolved UO_2 on either the viscosity or oxidation behavior of the melt. The heat of reaction for the dissolution of the UO_2 fuel by the molten Zircaloy is also unknown. All of these properties must be characterized before the melting and flow behavior of the cladding can be accurately modeled.

This report presents the significant program results and discusses these in terms of modeling the small-break LOCA accident. Specifically, the results discussed here include: 1) oxidation kinetics of Zircaloy and Zircaloy-UO_2 mixtures in steam and steam-hydrogen gas mixtures at 1300 to 2400°C, 2) viscosity measurements on zirconium-UO_2 mixtures at 1800 to 2100°C, 3) heat of dissolution data for UO_2 in zirconium at 1700 to 2000°C, and 4) thermal diffusivity measurements on prereacted Zircaloy-UO_2 mixtures at 800 to 1500°C.

EXPERIMENTAL PROCEDURE

Detailed descriptions of the experimental procedures used in these studies have been reported elsewhere (Prater and Courtright 1986, 1987; Bunnell and Prater 1986, Brimhall and Prater 1987). Therefore, only a brief description of each will be presented here.

OXIDATION KINETICS

A schematic of the oxidation apparatus is presented in Figure 1. A complete discussion of the experimental details is reported by Prater and Courtright (1987). The experiments were performed on disk specimens (3.8 mm diameter x 0.9 mm thick) that had been machined from reactor-grade Zircaloy-4 bar stock. A defocused CO_2 laser beam with a maximum power output of 400 W was used to heat the samples from one side. The surface temperature of the sample was measured using a two-color pyrometer calibrated at regular intervals against an internal radiation source and standardized to the melting point of alumina. Temperature measurements were considered accurate to within 15°C. The experimental configuration permitted placement of the pyrometer to view either the heated or the nonheated side of the sample. A computer was coupled to both the pyrometer output and the power control circuit of the CO_2 laser, thereby permitting rapid and reproducible temperature control to a preprogrammed time sequence. Oxidation experiments could be conducted in pure steam or in steam mixed with hydrogen, helium, or argon.

Isothermal oxidation experiments were performed between 1300 and 2400°C. The specimens were first heated to a predetermined temperature in argon. Preheated 600°C steam was then introduced through a fast-acting valve at a rate of 3 g/min. The ensuing oxidation resulted in a rapid rise to the desired temperature, which was then held at a constant level by controlling the laser-heat input. Each test was terminated after the desired time increment by closing the shutter on the laser, which resulted in a rapid quench of the sample at an initial rate of 500°C/s. Oxidation kinetics were determined by metallographically sectioning each sample and measuring the thickness of the ZrO_2 and α-Zr layers that formed.

VISCOSITY MEASUREMENTS

An oscillating-cup viscometer was used for conducting the viscosity measurements. This apparatus is shown schematically in Figure 2, and is described in detai' by Bunnell and Prater (1986), and Rasmussen et al. (1971). In this technique, a sealed container of the fluid is suspended from a torsion fiber and set into oscillation. The motion of the fluid causes a decay in the amplitude of the torsional oscillations of the pendulum, which can be related to the viscosity of the liquid. In the present study, a tungsten crucible with a thoria liner was used to contain the highly reactive molten Zircaloy and zirconium-UO_2 (5 to 30 mol% UO_2) mixtures. The temperature was measured with a Type C (W-5% Re versus W-26% Re) bare-wire thermocouple that was positioned to

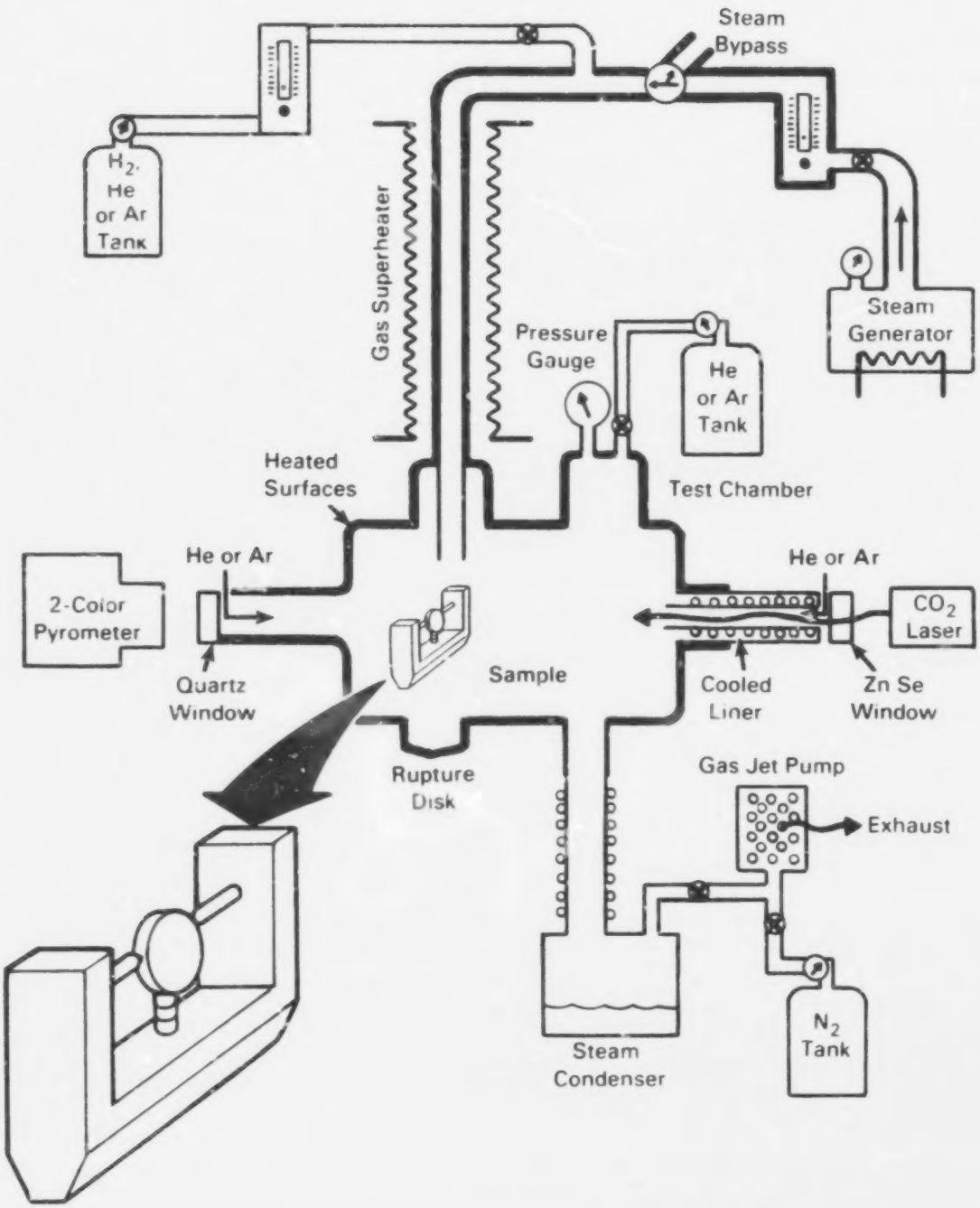

FIGURE 1. Apparatus Used to Measure High-Temperature Oxidation of Zircaloy

BEST COPY AVAILABLE

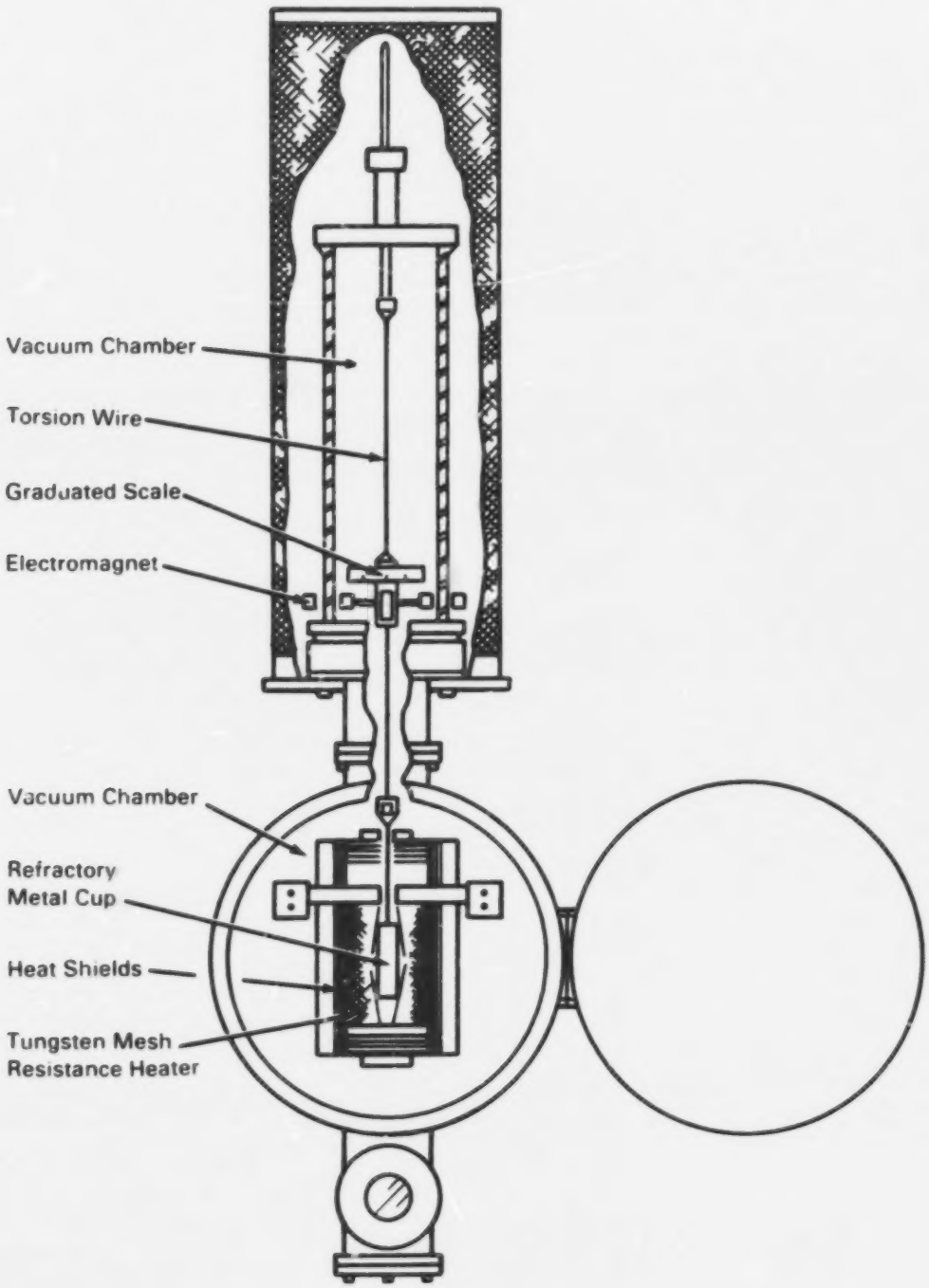

FIGURE 2. Oscillating-Cup Viscometer

BEST COPY AVAILABLE

within 0.6 cm of the bottom of the crucible. Because the thermocouple was not in actual contact with the sample, there was some uncertainty, estimated to be about 70°C, in the reporting of the sample temperatures. Viscosity measurements were conducted from 1700 to 2100°C.

HEAT OF REACTION MEASUREMENTS

The heat of reaction studies were performed using differential thermal analysis. This technique compares the heating or cooling behavior of the specimen with that of a reference sample. As the samples are heated (or cooled) through a temperature range where a reaction occurs in the specimen, its heating or cooling rate will increase or decrease as additional heat (associated with the heat of reaction) is either generated or absorbed. Comparison with the reference sample permits stray sources of external heat or noise to be discriminated from sources internal to the specimen. A schematic of the apparatus used in the present study is presented in Figure 3. A detailed discussion of the experimental approach is presented by Brimhall and Prater (1987). Briefly, the specimen and a reference material, in this case ZrO_2, were set side-by-side into a massive tungsten boat. Because of the corrosive nature of molten zirconium, ThO_2 crucibles were used to contain the

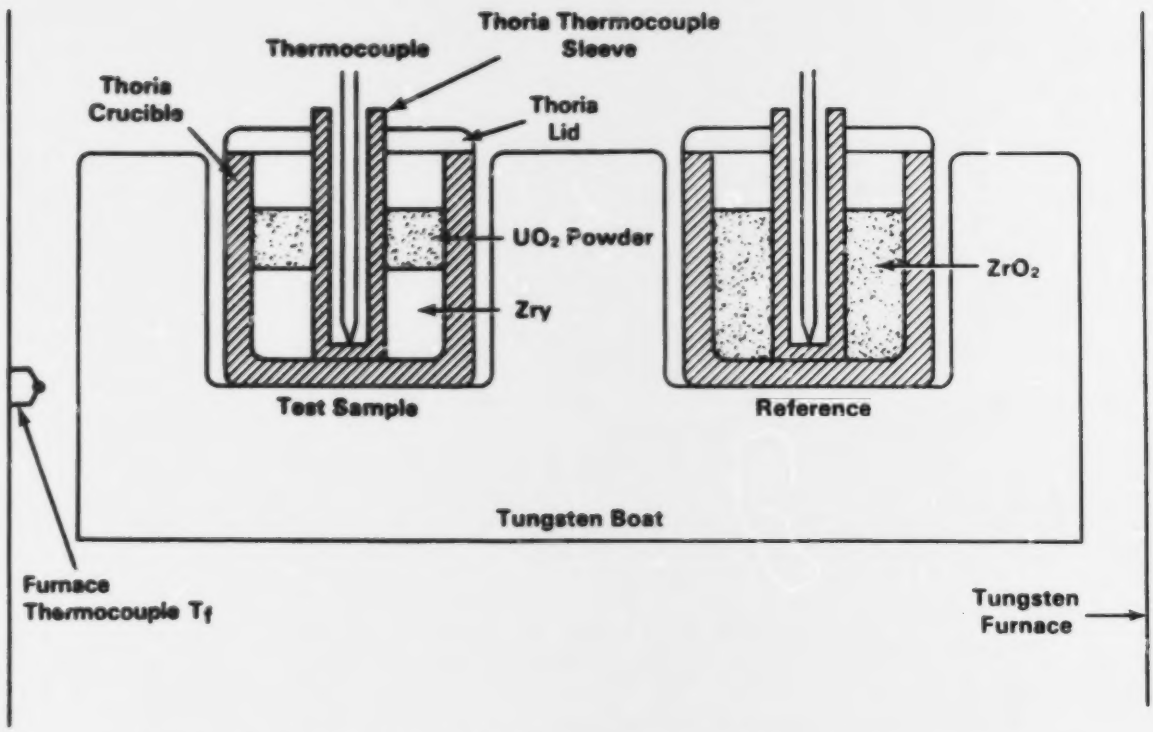

FIGURE 3. Schematic of the Apparatus Used to Measure the Heat of Reaction Between Zirconium and Uranium Oxide

BEST COPY AVAILABLE

samples. Smaller ThO_2 tubes were fused to the inside of the larger crucibles to accommodate a (type C) W-Re thermocouple. The sample (2 to 5 g depending on the crucible size) and reference materials were placed in the annulus region of their respective crucibles. The weight of the ZrO_2 was adjusted to give a similar heat capacity to that of the sample.

The heat-of-reaction measurements were performed in a gettered argon atmosphere. The sample was heated at a rate of either 5 or 10°C/s to a maximum temperature between 1950 to 2000°C. The sample was held at this temperature for up to 30 min before cooling at a rate of 10°C/s. Zircaloy-4 was initially used as the sample material but pure zirconium was later used because it produced a sharper melting peak. To minimize interaction between the Zr and the UO_2 prior to zirconium melting, powdered UO_2 was spread on top of premelted Zr. By premelting the Zr, good initial contact was obtained with the thermocouple sleeve. This procedure also established a melting peak for calibrating the apparatus.

THERMAL DIFFUSIVITY MEASUREMENTS

The thermal diffusivity of Zircaloy samples containing 15 and 30 mol% UO_2 was measured at 800 to 1500°C using the pulse technique described by Parker et al. (1961). The samples were prepared by arc melting Zircaloy bar stock and UO_2 powder into an ingot from which disk samples (10 mm diameter x 0.75 mm thick) were machined. These samples were then mounted in an alumina holder located inside of a W cold-wall furnace that was evacuated and backfilled with gettered Ar. The thermal diffusivity was measured by heating one surface of the disk with a short heat pulse from a 25-j ruby laser. As the heat pulse passed through the sample, the temperature rise on the back surface was recorded with an InSb infrared detector. The time required for the back surface to reach one-half its maximum temperature was determined from the time-temperature curve. The thermal diffusivity (TD) was calculated using the relationship:

$$TD = \ell^2/t_{1/2} \qquad (1)$$

where ℓ was the sample thickness and $t_{1/2}$ was the half-rise time.

BLANK PAGE

RESULTS AND DISCUSSION

OXIDATION KINETICS

The oxidation of Zircaloy proceeds first by the transformation of the beta phase (the stable high temperature phase of the pure alloy) to the alpha phase (stabilized by the dissolution of large amounts of oxygen in the metal) and then finally to the formation of the oxide. The oxidation kinetics were determined by measuring the rate of thickening of the oxide and alpha layers at 100°C intervals for temperatures between 1300 and 2400°C. Parabolic growth kinetics were found to apply over the entire temperature range studied and can be described by the kinetic expression:

$$k = \delta_k t^{1/2} \tag{2}$$

where k = a kinetic parameter (oxide thickness, ϕ; alpha-layer thickness, α; combined oxide and alpha-layer thickness, ξ; or total oxygen consumed, τ)

δ_k = parabolic rate constant

t = reaction time.

A linear relationship was observed for the thickening of the reaction layers versus the square root of time. This confirmed that the Zircaloy-steam reaction obeyed parabolic kinetics, indicating that the reaction was probably controlled by anion diffusion through the oxide. To further test this conclusion, experiments were performed where the oxidation kinetics were compared among samples exposed to different steam flow rates (from 3 to 18 g/min) and to steam pressures of 0.1 and ~0.5 MPa (1 and 5 atm absolute). No change in oxide-growth rates was observed, indicating that the reaction was not gas-phase diffusion limited.

Isothermal Oxidation Kinetics

The temperature dependence of the growth constants for the ZrO_2 and the combined layer (oxide and alpha layers) thicknesses are presented in Figure 4. The data measured on the laser-heated and nonheated surfaces of the sample produced two distinct curves with approximately the same slope and activation energy. Depending on the experimental configuration adopted, a temperature gradient was produced across the sample thickness which either decreased or increased, respectively, away from the isothermally controlled surface temperature. The exact profile of the temperature gradient across the sample could not be determined because the distribution of the heat from the oxidation reaction was not known. However, the temperatures on the two faces were measureable and the temperature gradient varied in proportion to the oxide thickness; each 100 μm of oxide thickness produced a temperature drop of about 50°C across the sample. The two data curves shown in Figure 4 represent the actual measured temperature at the oxide surface for the two heating geometries.

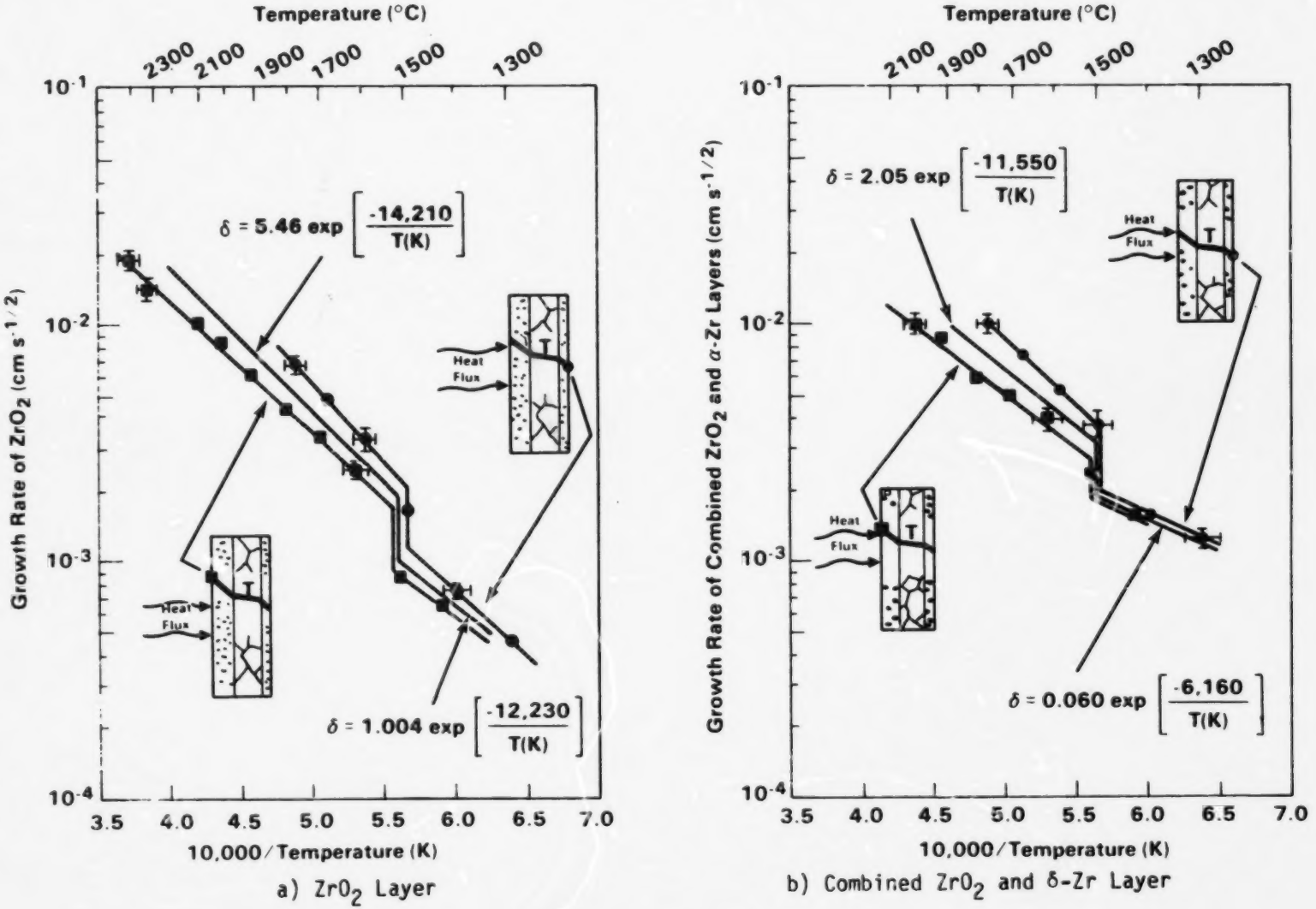

FIGURE 4. Parabolic Rate Constants for Oxide Layer Growth

BEST COPY AVAILABLE

The best estimate for the true isothermal oxidation rate, where no temperature gradient exists across the oxide layer, was the bisector of the two data curves. This was verified in an experiment where the laser beam was split and the two beams were directed so that both sides of the sample were heated simultaneously. Although experimental difficulties (beam alignment and focusing) still resulted in a small deviation from true isothermal conditions, the oxidation kinetics fell between the two original data sets, as expected.

As previously reported by Urbanic and Heidrick (1978), a discontinuity occurs in the oxide growth rate at approximately 1500°C. This discontinuity is associated with the development of the cubic (high-temperature) oxide phase, shown in Figure 5. No other discontinuity in growth rate was observed, either upon melting of the underlying metal at 1980°C or upon transformation of the duplex (tetragonal-cubic) ZrO_2 layer to a single-phase cubic oxide at 2370°C

FIGURE 5. Micrograph of Zircaloy-4 Oxidized in Steam for 40 s at 1595°C

BEST COPY AVAILABLE

(Levin and McMurdie 1975); see Figure 6. No other phase transitions occur in the zirconium-oxygen system up to the melting temperature of ZrO_2 at 2680°C. Thus, the data for ZrO_2 growth can probably be extrapolated up to 2680°C without major error.

Total oxygen consumption was estimated from the layer growth rate data. By measuring the sample weight gain and estimating (metallographically) the quantities of oxide and alpha zirconium that formed in selected samples, it was possible to approximate the oxygen densities for the different phases. Oxygen dissolution in the beta-zirconium layer was assigned only to the alpha layer. This resulted in values of 1.53 mg O_2/mm^3 for ZrO_2 and 0.5 mg O_2/mm^3 for α-Zr.

The temperature dependence of the isothermal growth constants obtained from Zircaloy-4 above 1510°C for the ZrO_2 layer (δ_ϕ), the combined layer (δ_ξ), and total oxygen consumption (δ_τ) can be described by the following equations:[a]

$$\delta_\phi^{Zry\text{-}4} = 5.46 \exp [-14210/T(K)] \ (\pm 35\%) \ cm\text{-}s^{-1/2} \quad (T = 1510 \text{ to } 2400°C)$$
$$\delta_\xi^{Zry\text{-}4} = 2.05 \exp [-11550/T(K)] \ (\pm 42\%) \ cm\text{-}s^{-1/2} \quad (T = 1510 \text{ to } 1900°C) \qquad (3)$$
$$\delta_\tau^{Zry\text{-}4} = 5.74 \exp [-13220/T(K)] \ (\pm 40\%) \ g/cm^2\text{-}s^{-1/2} \quad (T = 1510 \text{ to } 2400°C)$$

The ZrO_2 growth rates determined in this study are compared with those of Cathcart and Pawel (1977), Urbanic and Heidrick (1978), and Baker and Just (1962) in Figure 7. For temperatures below 1500°C, the Cathcart-Pawel curve correlates well with at least six other studies.[b] Above 1510°C, the kinetics increase to rates slightly above those reported by Baker and Just. The discontinuity in kinetics coincides well with the transformation temperature of 1490°C where cubic ZrO_2 becomes stable (Ruh and Garrett 1967), shown in Figure 6. There are differences between the data from this study and those of Urbanic and Heidrick (1978) both for the rate curves above 1500°C and the temperature at which the discontinuity in the growth kinetics occurs. These differences cannot be easily explained without detailed knowledge of the experimental procedures used by Urbanic and Heidrick and possibly by assuming some uncertainties in the temperature measurements.

Effect of Temperature Gradients

In applying the rate equations to the modeling of a fuel rod during a LOCA, consideration must be given to the heat flux within the rod. For example, actual oxidation rates might be better approximated by biasing the rates

---

(a) The uncertainties in the constants (±35, 42, and 40%) were determined by establishing 95% confidence limits for the data shown in Figure 4 and determining the uncertainty in the bisector from extreme values of the experimental curves.

(b) Cathcart and Pawel 1977; Hobson and Rittenhouse 1972; Suzuki, Kawasaki, and Furuta 1977; Ikeda, Ito and Ohashi 1975; Leistikow, Shanz, and V. Berg 1978; Biederman et al. 1976; Sawatsky, Ledoux and Jones 1977.

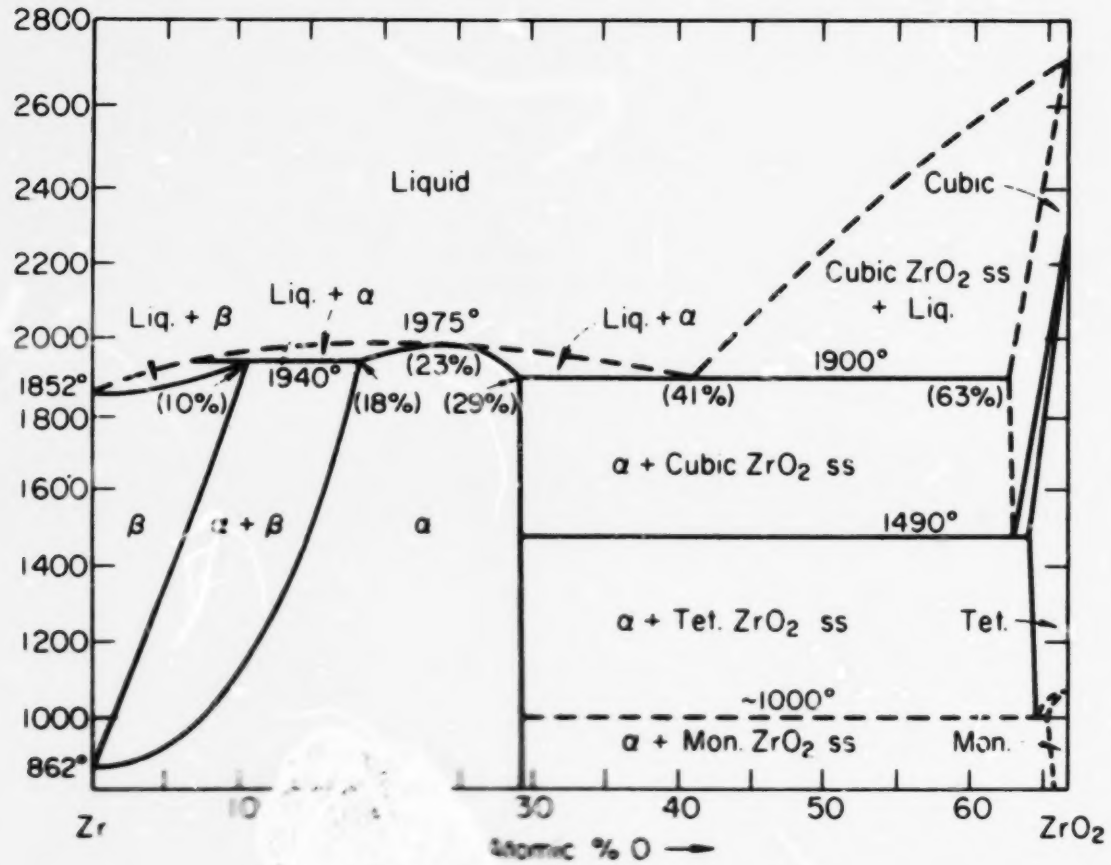

Zirconium-Oxide Phase Diagram

towards the experimental [illegible] from samples with the temperature gradient similar to that of the fuel rod being modeled. A detailed heat balance within the cladding cannot be performed because the distribution of heat generated by the oxidation reaction is not known. However, to first approximation, the heat of oxidation can be disregarded because it is contained intrinsically within the experimental data. By doing this, the major consideration becomes one of calculating the relative contributions from the supplemental heat sources, i.e., the fission product decay heat of the fuel and the heat being radiated from neighboring rods. When internal heating dominates, the rates will approach those of the upper curve. This is certainly the case at the start of an accident when the decay heat of the fuel is the major source of heat. Later, as rod-to-rod radiation becomes a major contributor, rates should drop closer to the lower curve.

A correction to the oxidation rate equations to account for the effect of the temperature gradient across the oxide can be incorporated into the oxidation models by multiplying the parabolic rate constants (Equation 3) by the following:

BEST COPY AVAILABLE

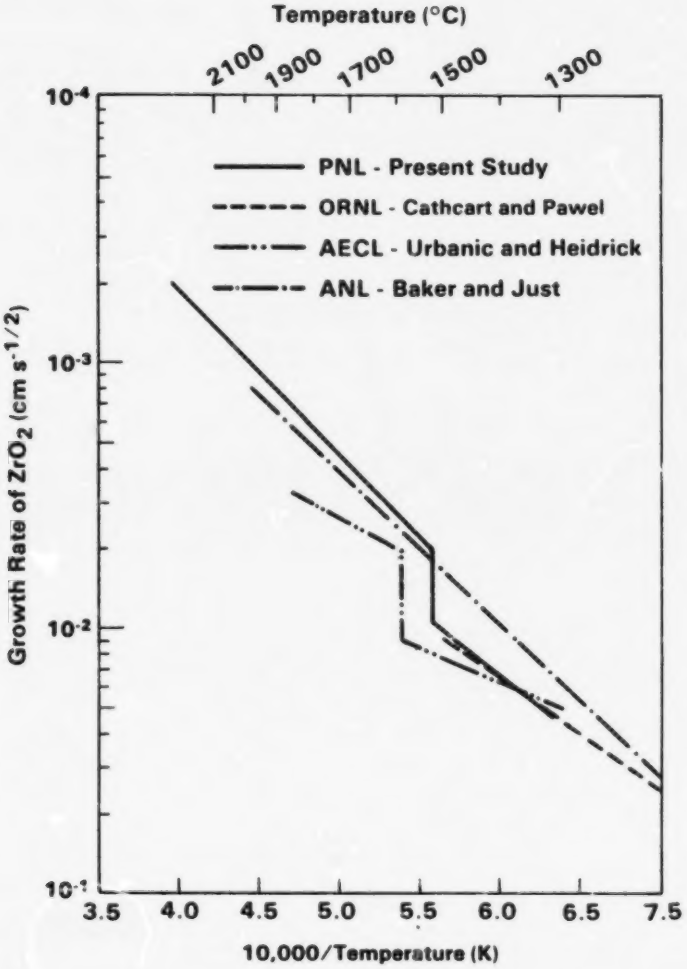

FIGURE 7. Comparison of Parabolic Rate Constants for Oxide Layer Growth

$$\sigma = 1 + 0.3 \quad (H_i - H_e)/(H_i + H_e) \qquad (4)$$

where H_i is the sum of all the heat that enters the oxide volume through the oxide-metal interface, e.g., the heat that originates from fission product decay in the fuel or heat conduction along the rod length; and H_e is the sum of all the heat that enters the oxide layer through the oxide-gas interface, e.g., rod-to-rod radiation. The heat derived from the oxidation reaction within the cell of interest is not included in these summations.

BEST COPY AVAILABLE

Application to Transient Oxidation

The validity of using isothermal rate equations to model a transient problem, such as the oxidation of the cladding during the rapid heating and cooling cycle that is experienced during a LOCA, was studied by analyzing the results of five different heating and cooling experiments. A description of each transient experiment is provided in Table 1.

The thicknesses of the oxide layers that formed on each sample were measured and compared with the predictions of a model using isothermal growth rate constants for oxidation on the nonheated side of the sample (the test geometry used for the experiment). For modeling, each transient was broken down into a series of discrete isothermal steps. The calculation accumulated the oxide and combined layer thicknesses at each step along the transient. To determine incremental growth rates, prior oxide growth was calculated from an equivalent time at temperature. This represented the time the sample would have to have been held isothermally at the specified temperature to reach the combined layer thickness. The incremental growth of the respective layers formed during the specified time interval could then be calculated and added to the thicknesses already present. This process was repeated until the entire transient had been analyzed.

TABLE 1. Comparison of Computed and Measured Layer Thicknesses Formed During Transient Oxidation

Run #	Transient Experiment	ZrO_2 Thickness (μm) Measured	ZrO_2 Thickness (μm) Computed	ξ Thickness (μm) Measured	ξ Thickness (μm) Computed
A	Heated in steam from 200 to 2059°C at 500°C/s, then cooled from 2059° to 1650°C at 100°C/s	290	312	*	-
B	Steam added while sample held at 1400°C for 10 s, then ramped to 1700° at 5°C/s	227	238	387	365
C	Steam added while sample held at 1400°C for 300 s, then ramped to 1550°C at 10°C/s	176	146	412	297
D	Sample held at 1520°C for 120 s, then cooled to 1400°C at 10°C/s	249	260	*	-
E	Sample held at 1520°C for 120 s, then cooled to 1400°C at 1°C/s	316	295	*	-

* overlapping α-layers

There was good agreement, ±8%, between the computed and measured values for all but one of the samples, see Table 1. The exception was experiment C in which the sample spent an extended time below the 1510°C transition temperature and only 4 s above. The model was not able to account for the redistribution of oxygen between the metal and the oxide that occurs upon heating through the phase transformation at 1510°C. As a result the model underestimated the thickness of the oxide layer by about 20%, and the thickness of the combined layer by almost 40%.

One method for realistically modeling the growth of the oxide layers at temperatures near the ZrO_2 transition temperature (around 1500°C) would be to treat it as a moving boundary diffusion problem and track the diffusion of the oxygen within the cladding. However, this calculation was felt to be beyond the scope of the current program.

Oxidation of Zircaloy-Uranium Oxide Mixtures

Zircaloy samples with 15 mol% UO_2 were prepared by arc melting Zircaloy bar stock and UO_2 powder into a slug from which the standard-sized disk samples were machined. Isothermal oxidation experiments were performed at 1415, 1820, and 2140°C. Measurements were performed on the laser-heated side of the samples. An adjustment was then made to correct for the heating geometry based on the previous results for Zircaloy. The starting samples consisted of multiple phases: an oxygen-saturated α-Zr phase, a uranium-rich metallic phase at the α-Zr grain boundaries, and a UO_2-rich phase. These are the equilibrium phases that were expected based on the ternary phase diagram studies by Skokan (1984).

Oxidation of this alloy proceeded preferentially with the formation of a uranium-rich phase either along the U-enriched grain boundaries in the solidified alloy or as stringers extending out into the molten metal mixture in advance of the α-Zr/ZrO_2 interface. In either case, the result was the growth of an oxide layer that consisted of two phases: a uranium-rich oxide (45 to 90 mol% UO_2) phase, and a nearly pure ZrO_2 (containing less than 5 mol% UO_2) phase, as shown in Figure 8. The chemical analysis was performed in a scanning electron microscope equipped with an energy dispersive x-ray analyzer. Crystalline phase analysis by X-ray diffraction on the oxide at ambient temperatures indicated that the phases were cubic UO_2 and monoclinic ZrO_2. Apparently, the uranium content in the ZrO_2 was not sufficient to stabilize the cubic phase, although it may have depressed the transformation temperature.

The growth of the ZrO_2 layer again displayed parabolic kinetics. The temperature dependence of the growth constant for ZrO_2 layer thickness is presented in Figure 9. For comparison, the previous results obtained for oxide growth on the laser-heated side of Zircaloy samples are also presented. Above 1500°C the two curves are virtually identical. Interestingly, no discontinuity was observed in the Zry-UO_2 curve at 1500°C. After correcting for the heating geometry, the parabolic growth constants in a Zr-15 mol% UO_2 mixture for the

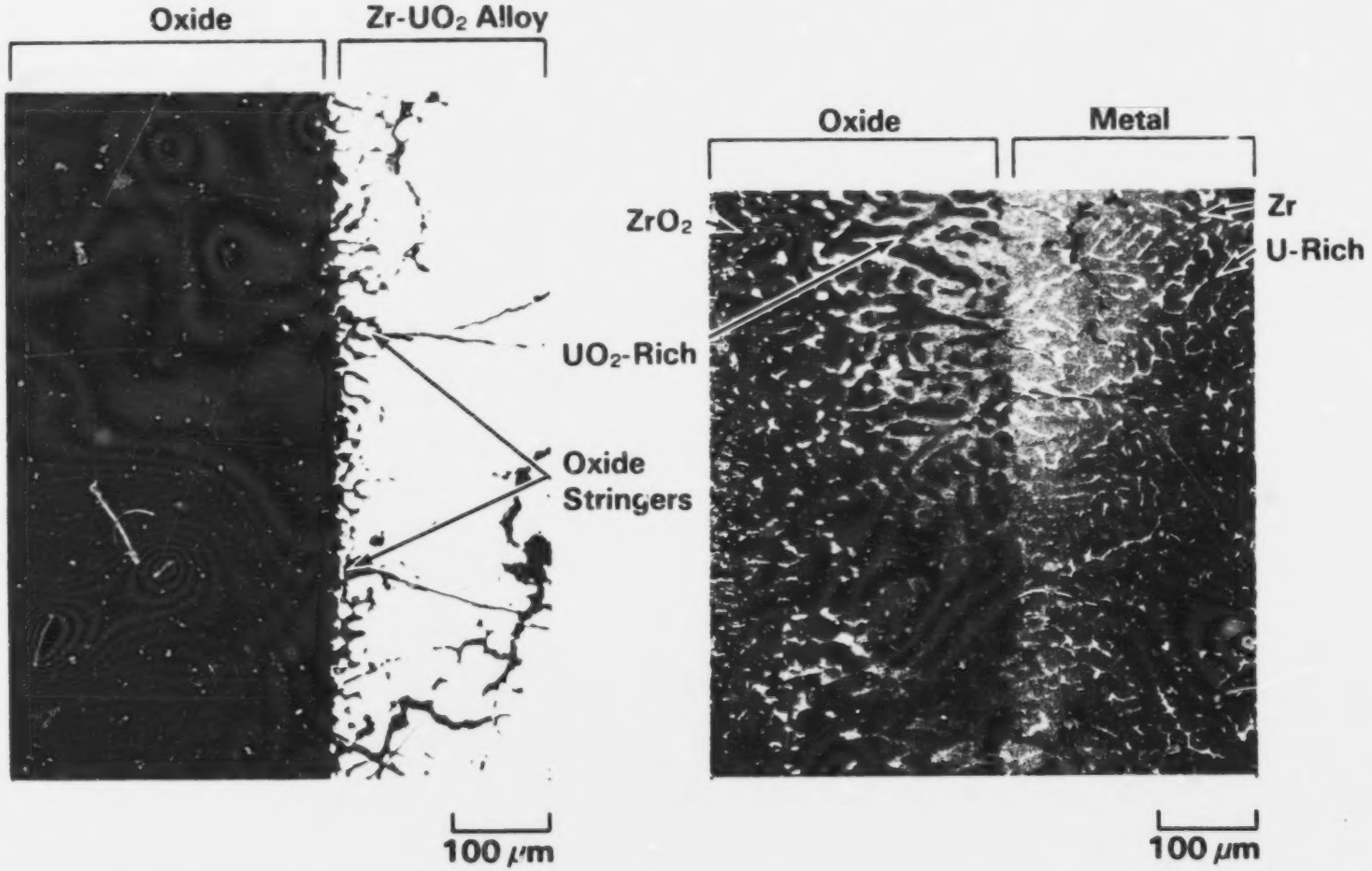

FIGURE 8. Micrograph of a Zircaloy-15 mol% Uranium Oxide Sample Oxidized in Steam for 27 s at 1820°C Showing Preferential Oxidation of the Uranium-Rich Phase

BEST COPY AVAILABLE

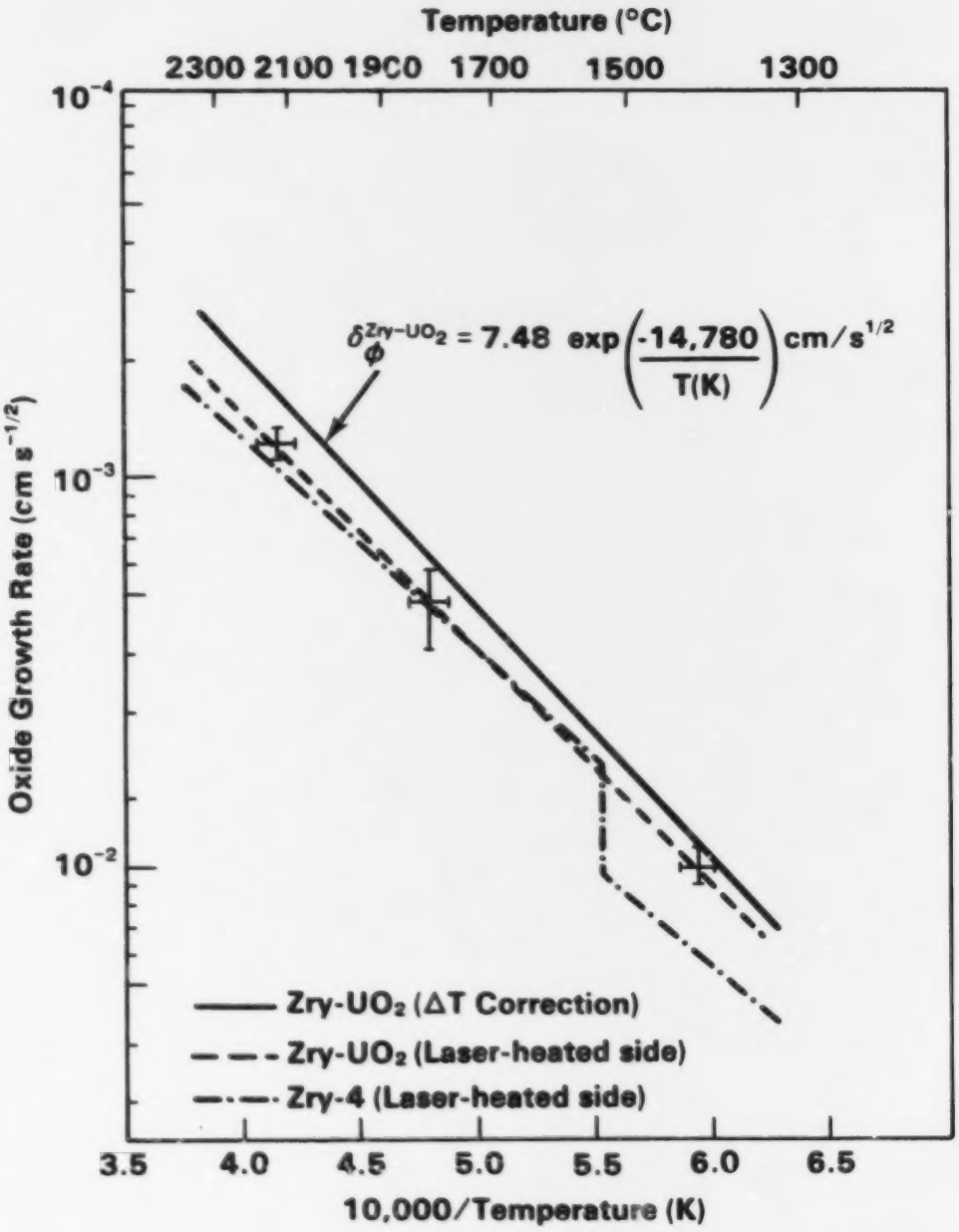

FIGURE 9. Isothermal Parabolic Rate Constant for Oxide Layer Growth on Zirconium-15 mol% Uranium Oxide

BEST COPY AVAILABLE

ZrO_2 layer thickness (δ_ϕ) and total oxygen consumption (δ_τ) were found to be described by the following equations:[a]

$$\delta_\phi^{Zry\text{-}UO_2} = 7.48 \exp(-14780/T(K)) \quad (\pm 35\%) \text{ cm-s}^{-1/2}$$

$$\delta_\tau^{Zry\text{-}UO_2} = 9.13 \exp(-14780/T(K)) \quad (\pm 38\%) \text{ g oxygen - cm}^{-2} \text{ - s}^{-1/2} \qquad (5)$$

where T = 1400 to 2150°C

Effect of Steam Dilution by Hydrogen

During a LOCA, large quantities of hydrogen can evolve as a by-product of the oxidation reaction. Previous studies suggested that a significant reduction in the oxidation rates (by as much as 80%) occurred as the hydrogen concentration in the gas phase increased above 50 mol% (Chung and Thomas 1981). More recent work raised the concentration limit to 70 mol% hydrogen (Chung and Thomas 1983).

To better characterize this phenomenon, oxide thickness measurements were performed on a series of samples exposed to different steam-hydrogen mixtures under equivalent temperature transient conditions. The results are presented in Figure 10. For these experiments, a constant steam flow rate of 3 g/min was maintained and the hydrogen flow was varied to provide the desired H_2/H_2O ratio. This helped to assure that the supply of steam to the sample was maintained at an adequate level to support the oxidation requirements; i.e., that steam starvation was not inadvertently induced, as a result of the gas mixing, and then mistakenly identified as a hydrogen effect.

All of the samples exposed to the steam-hydrogen mixtures (5 to 100 mol% steam) for 25 s at 1565°C developed equivalent oxide thicknesses, as shown in Figure 10(a). Oxide growth was inhibited only in pure hydrogen. The small rise in the curve at the higher hydrogen contents was a result of sample cooling by the hydrogen gas. This cooling steepened the temperature gradient across the sample and increased the oxidation rate slightly on the nonheated side of the sample where oxide growth was being monitored in this experiment.

At 1815°C, the oxidation kinetics dropped sharply when the concentration of steam decreased to below 8%, as shown in Figure 10(b). However, a mixture of 9% H_2O and 91% He exhibited a similar decrease in kinetics, suggesting that the supply of steam to the sample surface (gaseous transport) may be limiting the kinetics at these high dilutions. Mass transfer coefficients in the gas phase are flow dependent (Bennett and Meyers 1962). At the higher gas flow rates used to obtain the more dilute steam mixtures, steam supply to the sample surface may have been insufficient to satisfy full rate oxidation at 1815°C and

(a) The uncertainties in the rate constants (±35% and ±38%) were based on the analysis performed earlier for the Zircaloy oxidation experiments, see page 12.

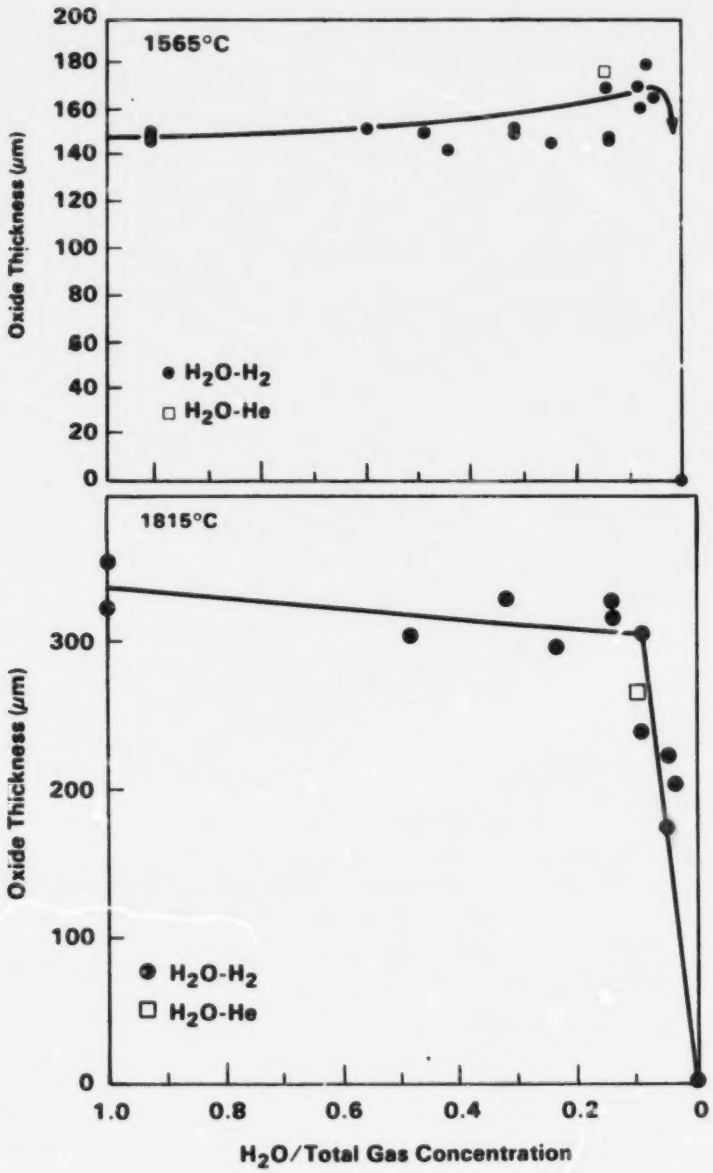

FIGURE 10. Effect of Hydrogen on Oxidation Kinetics

thereby caused a decrease in the oxide thickness. Thus, the rapid decrease in oxidation does not appear to be uniquely caused by hydrogen but resulted from a more general gas dilution effect.

As the hydrogen concentration was increased, the cooling effect of the hydrogen-rich gas mixtures again increased the temperature gradient across the sample. However, because the 1815°C experiments were conducted on the laser-

BEST COPY AVAILABLE

heated side of the sample, the oxidation rate decreased slightly as the gas composition was varied from 0 to 90% hydrogen.

One other experiment was performed to determine the effect that prior hydrogen loading of a sample had on its subsequent oxidation behavior at 1800°C. Zircaloy samples were first heated to 1100°C in pure hydrogen and held for 80 s. This resulted in dissolution of approximately 30 at.% (0.5 wt%) hydrogen in the Zircaloy metal. These samples were then oxidized in different steam and steam-hydrogen mixtures at 1800°C and the rate of oxide layer growth was compared with non-hydrogen-loaded samples. The oxidation kinetics were lower in all the hydrogen-loaded samples by about 20%. The greatest difference was the formation of large amounts of porosity in the tetragonal ZrO_2, which made this layer extremely brittle and prone to spallation during cooling.

Hydrogen analysis was performed on fourteen representative samples by Oregon Metallurgical Corporation. The total concentration of hydrogen dissolved in the individual samples was determined using the inert-gas fusion technique. The results are presented in Table 2. Zircaloy samples that had been oxidized in pure steam had hydrogen contents that were roughly 1 at.%. Those samples that had been oxidized in steam-hydrogen mixtures varied from 1 to 10 at.%. By far the greatest hydrogen uptakes, between 30 and 40 at.%, were measured in those samples that had been exposed to pure hydrogen or preloaded with hydrogen prior to oxidation. The presence of an oxide surface layer significantly blocked the diffusion of hydrogen into the Zircaloy samples.

Differences between the present results and those reported by Chung and Thomas (1981, 1983) are difficult to resolve without detailed knowledge of the experimental procedures used by Chung and Thomas. However, it appears that many of the Chung and Thomas experiments may have been performed under steam-deprived conditions. Also, in the Chung-Thomas experiments, the samples were heated to test temperature in a hydrogen-bearing environment rather than the inert-gas atmosphere used in the present study. Thus, in the Chung-Thomas experiments, significant hydrogen dissolution may have occurred during initial

TABLE 2. Hydrogen Analysis for Oxidized Zircaloy-4 Samples Using the Inert-Gas Fusion Technique

Sample Description	Number of Samples Analyzed	Total H_2 Content
A. Samples oxidized in pure steam 1500-2300°C	6	1 at.% H_2 (0.02 wt%)
B. Samples oxidized in steam-hydrogen mixtures (85-95% H_2) at 1560 and 1800°C	4	5-10 at.% H_2
C. Samples precharged with H_2 (to 30 at.%) and then oxidized in steam-hydrogen -20% slower oxidation kinetics	4	35 at.% H_2

heating when only a thin oxide layer would have been present on the sample surface. It is believed that these experimental differences may account for the apparent discrepancy in the reported results for these two studies.

With respect to a LOCA, hydrogen effects do not appear to represent an important consideration. During the early stages of a LOCA there will not be much hydrogen present in the atmosphere. It is not until the LOCA is well under way and temperatures in the majority of the uncovered core have reached 1200°C or more that a significant fraction of hydrogen is present in the atmosphere. Thus, during the heating transient of a LOCA, the oxidation kinetics should progress at full rate, as indicated by the present work, until steam-starved conditions develop and oxidation ceases.

In all likelihood, the hydrogen content of the cladding will remain low throughout the transient, since thick oxide layers will have already formed on the cladding prior to the generation of a hydrogen-rich atmosphere. As long as the hydrogen content of the cladding remains low, oxidation rates will not be affected. The notable exception might be if cladding rupture occurs rather late in the transient and exposes an unreacted inner cladding surface to a pure hydrogen atmosphere. Then, significant dissolution of hydrogen could occur which would be expected to slow subsequent oxidation of the cladding, most notably during core reflood, by about 20%.

VISCOSITY OF ZIRCONIUM-URANIUM OXIDE MIXTURES

Viscosity values for molten Zircaloy-2 and Zr-UO_2 mixtures containing up to 30 mol% UO_2 are presented in Figure 11. There is almost no dependence of viscosity on UO_2 content over the composition range studied. The viscosity values remained nearly constant between 10 and 17 centipoise. For comparison, water has a viscosity of 1 centipoise and 10W motor oil has a viscosity of about 2000 centipoise at room temperature.

Contamination of the molten samples by the thoria crucibles was minimal. Analyses of the metal in the viscosity samples heated to 2150°C were performed by inductively coupled plasma atomic absorption spectroscopy. These analyses indicated that the amount of dissolved thorium was less than 1 mol% for most experiments and should not have influenced the results.

The apparent melting temperature at which fluid flow was first observed generally rose with increasing UO_2 content, as shown in Figure 12. The viscosity experiments defined three temperature regimes for each Zr-UO_2 mixture: 1) a temperature below which the mixture was always solid, 2) an intermediate temperature where the sample was apparently a mixture of solid and liquid phases and where the viscosity was poorly defined, and 3) a temperature above which the samples were always molten and had a viscosity between 10 and 17 centipoise. The observed melting temperatures and final microstructures were in general agreement with the existing phase diagram studies by Skokan (1984). Unfortunately, the tie line connecting pure Zr to UO_2 in the Zr-U-O ternary phase diagram has not been well characterized above 1900°C making quantitative comparison difficult. However, it does appear that all of the Zr-UO_2 samples

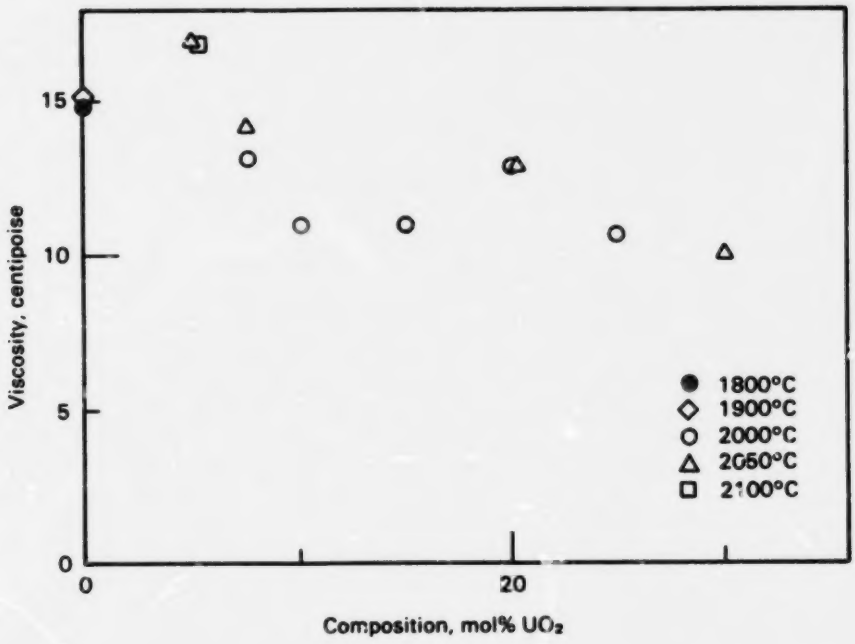

FIGURE 11. Calculated Viscosity Values for Zircaloy-2 and Various Zirconium-Uranium Oxide Mixtures as a Function of Composition

existed as a mixture of solid and liquid phases prior to complete melting. In this state, the mixture could show either solid or liquid behavior depending on the relative concentrations of the solid and liquid phases, the shape of the solid particles, and the shear force imposed on the mixture itself.

The compositions containing greater than 15 mol% UO_2 exhibited a temperature hysteresis in the viscosity data between the initial heating and all subsequent cooling and heating cycles. The reason for the hysteresis was not definitely established, although a change in microstructure that resulted from initial melting and resolidification appeared to be responsible. The hysteresis can be explained by assuming that fluid flow occurred prior to complete dissolution of the solid particles upon initial heating. The solid phases were originally present as powders. Small amounts of undissolved spherical particles would interfere only slightly with the flow of the molten liquid phase. Therefore, it is likely that the mixtures were displaying fluidity before they were completely molten.

After heating, molten samples with greater than 15 mol% UO_2 developed a pronounced dendritic oxide phase that could be seen in the resolidified microstructure (see Figure 13). It can be hypothosized that these dendrites, which develop an interlocking structure, would strongly interfere with the flow of the mixture and produce a semisolid mixture with high viscosity. Even the presence of a small fraction of dendritic solid phase would be enough to freeze

BEST COPY AVAILABLE

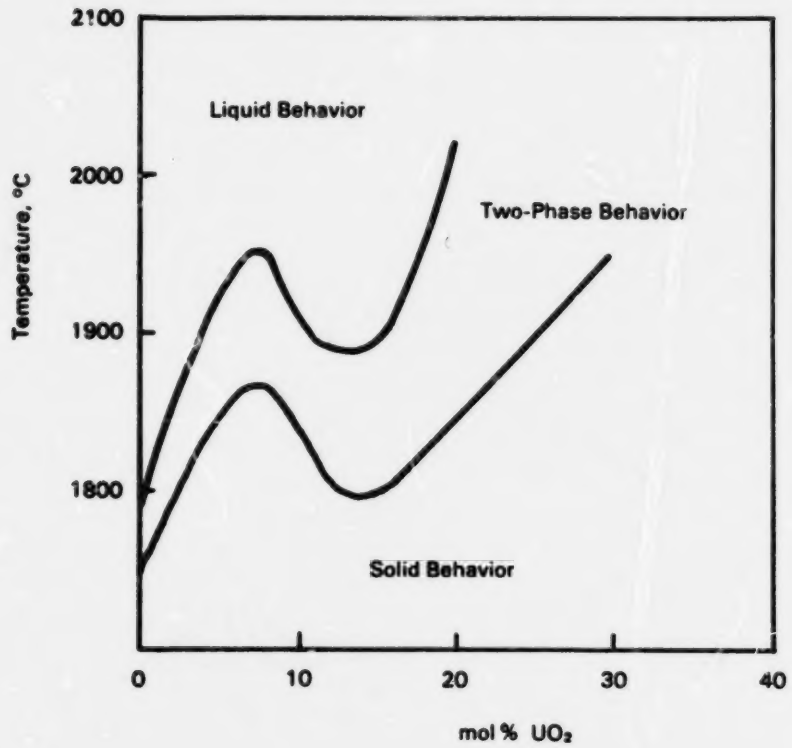

FIGURE 12. Schematic Diagram of Flow Behavior as a Function of Temperature and Uranium Oxide Content

the mixture. Upon subsequent heating, fluid flow would be delayed until the dendritic structure was completely dissolved, i.e., until the melting temperature was reached. Hence, the change in microstructure that occurred upon initial melting of Zr-UO_2 powder mixtures with greater than 15 mol% UO_2 could explain the observed hysteresis in the viscosity versus temperature data.

The torsion pendulum technique used in this study was not well suited for fully characterizing multicomponent fluids since only the lowest range of shear forces could be studied. Viscosities for slurry mixtures are very much shear-dependent. However, the values derived for the viscosity of the Zr-UO_2 mixtures in the present study should be valid for low shear conditions, as is the case for a liquid flowing downward under its own weight. This is the situation of greatest interest in modeling a LOCA.

The melting of the cladding during an LOCA and subsequent flow downwards is a difficult phenomena to model. As the fuel rod begins to heat, some dissolution of the UO_2 by the Zircaloy cladding would occur. The extent of this solid state interaction would depend strongly on the contact pressure that exists between the fuel pellets and the cladding (Hofmann, Kerwin-Peck, and

BEST COPY AVAILABLE

FIGURE 13. Micrograph of a Zr-30 mol% Uranium Oxide Sample After Heating to 2100°C

Nikolopoulas 1984). As the cladding temperature increases above 1780°C the cladding would begin to melt. Zircaloy melts at 1780°C; β-Zr melts at 1850 to 1940°C, depending on the oxygen content of the metal; and α-Zr melts at 1900 to 1975°C. Thus, melting would begin at the middle of the cladding thickness in the areas of lowest oxygen content and then spread, both outward and inward. Above 1980°C, all of the metal would exist as a single molten phase, which would be held in place by a shell of ZrO_2 that formed on the outside of the cladding. At this point, the molten Zircaloy would be in intimate contact with the solid fuel pellets and dissolution of the UO_2 would proceed rapidly. Reaction rates have recently been measured by Hofmann and Politis (1979).

At some point, the oxide shell would rupture releasing the superheated liquid. The breach in the oxide shell could be initiated by several means: 1) overpressure as the height of the molten metal reservoir increases with continued melting of the cladding, 2) dissolution of the oxide by unsaturated zirconium metal, or 3) other occurrences such as system vibrations or impacts by miscellaneous debris. The molten metal would then flow down the rod, much like wax dripping down a candle, until it cooled to below its melting point (the upper line in Figure 12) and solidified. The resolidification temperature would be composition dependent, and would therefore depend strongly on the length of time the molten cladding was in contact with the UO_2 fuel.

BEST COPY AVAILABLE

HEAT OF REACTION FOR DISSOLUTION OF URANIUM OXIDE BY MOLTEN ZIRCONIUM

An estimate of the heat of reaction for UO_2 dissolution by Zircaloy was obtained from a series of differential thermal analysis (DTA) experiments. In this technique, thermocouples record the temperatures of the reference and the sample. By connecting these in opposition, very small temperature differences between the sample and reference material can be detected. The sensitivity is great because all external contributions to the temperature measurement and fluctuations in the heating rate cancel. The temperature deviations of interest are those that result when a reaction or transformation occurs in the sample and are accompanied by the generation or consumption of a small amount of heat. By comparing the sample temperature with that of the reference material, temperature deviations (phase transformations or reactions) can be readily identified and a heat of reaction calculated.

In our Zr-UO_2 experiments, the DTA became extremely noisy above 1800°C. This coincided with the gradual rise in the electrical conductivity of the thoria crucibles. As the thoria became conductive, the DTA was transformed into a small electrochemical cell with each thermocouple in effect becoming an electrode. A stray emf was generated between the reference and test materials that was not easy to distinguish from the thermocouple emf. As a result, the baseline began to drift and the whole system became noisy. This necessitated that the measurement be performed with the two thermocouples completely isolated from one another, which reduced the sensitivity of the measurement.

Despite the reduced sensitivity the thermal peaks associated with Zr melting (P1), Zr-UO_2 reaction (P2), and Zr-UO_2 solidification (P3) could be resolved, as seen in Figure 14. Derivation of an actual heat of reaction was further complicated by the fact that an unknown amount of oxygen dissolution occurred prior to the reaction peak (P2). While the sample was being heated to temperature there was some interaction between the zirconium and the UO_2 layers. In addition, the UO_2 formed a sintered mass while it was being heated which slowed the rate of the reaction when the zirconium melted.

The observed reaction peak is believed to have been produced when the UO_2 finally disintegrated and dropped into the Zr. Since some dissolution occurred prior to the disintegration, the mass of UO_2 that actually dissolved during this final stage could only be estimated.

For purposes of calculation, it was estimated that only about 35% of the UO_2 had reacted with the Zr before the UO_2 disintegrated. This meant that the reaction peak corresponded to the dissolution of approximately 16 wt% UO_2. The heat of reaction was, therefore, calculated to be 20 (±10) kcal/mol UO_2 and was exothermic. In terms of the LOCA, this represents a pretty small contribution to the total heat input. At 2000°C the heat generated by steam oxidation of the cladding is 140 kcal/mol Zr.

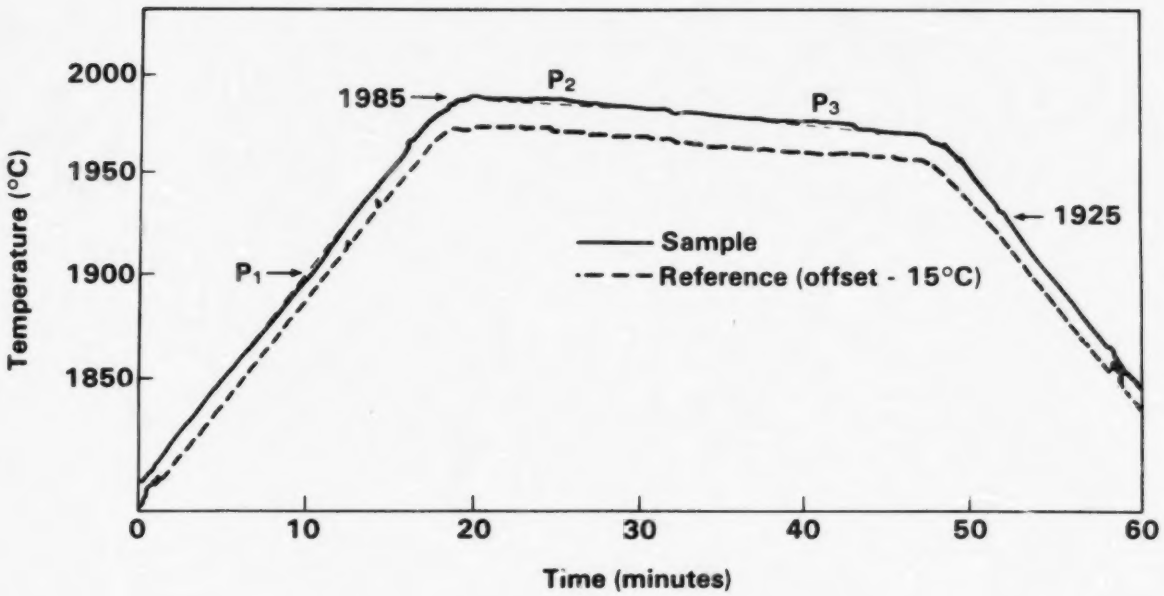

FIGURE 14. Thermal Analysis Curve for Zirconium-25 wt% Uranium Oxide

THERMAL DIFFUSIVITY OF ZIRCALOY-URANIUM OXIDE MIXTURES

Thermal diffusivity measurements were performed at 800 to 1500°C on pre-reacted Zircaloy-UO_2 samples containing 15 and 30 mol% UO_2. The results are presented in Figure 15. Previously reported results for Zircaloy-4 (Bunnell et al. 1977) and UO_2 (Bates 1970) are presented for comparison. The Zircaloy-UO_2 samples have thermal diffusivities that fall between the values for the pure Zircaloy and UO_2. Above 1723 K the samples started to oxidize and the values began to drop. At this point, the experiments were terminated.

BEST COPY AVAILABLE

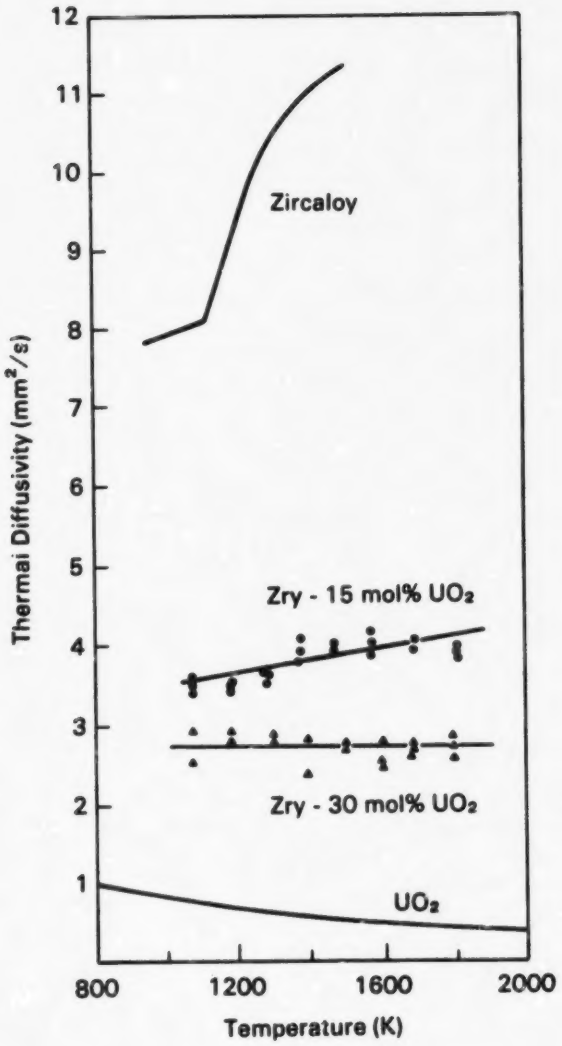

FIGURE 15. Thermal Diffusivity Measurements for Prereacted Zircaloy-Uranium Oxide Mixtures

BEST COPY AVAILABLE

SUMMARY

The following conclusions are based on the research conducted under the Severe Core Damage Materials Property Tests Program:

- Oxidation rates in steam for Zircaloy-4 and Zircaloy-15 mol% UO_2 are comparable above 1500°C and are greater than those previously reported by Baker-Just and Urbanic-Heidrick.
- As long as the steam supply to the sample surface is sufficient to satisfy the oxidation requirements (steam starvation is not occurring) then changes in the gas flow rate, pressure, and composition (particularly H_2 content) do not affect the oxidation kinetics.
- The viscosity of molten Zircaloy-2 and Zr-UO_2 mixtures with 5- to 30-mol% UO_2 is between 10 and 17 centipoise.
- The heat of reaction for the dissolution of UO_2 by molten zirconium was difficult to measure, but was estimated to be about 20 Kcal/mol UO_2 (exothermic).
- Thermal diffusivity values of the Zircaloy-UO_2 mixtures (containing 15 to 30 mol% UO_2) are approximately 3 mm^2/s between 800 and 1500°C.

BLANK PAGE

REFERENCES

Baker, L., and L. C. Just. 1962. Studies of Metal-Water Reactions at High Temperature: III. Experimental and Theoretical Studies of Zirconium-Water Reaction. ANL-6548, Argonne National Laboratory, Argonne, Illinois.

Bates, J. L. 1970. High-Temperature Thermal Conductivity of 'Round Robin' Uranium Dioxide. BNWL-1431, Battelle Pacific Northwest Laboratories.

Bennett, C. O., and J. E. Meyers. 1962. Momentum, Heat and Mass Transfer. McGraw-Hill Book Co., Inc., New York.

Biederman, R. R., et al. September 1976. A Study of Zircaloy-4-Steam Oxidation Reaction Kinetics. EPRI NP-225, Electric Power Research Institute, Palo Alto, California.

Brimhall, J. L., and J. T. Prater. 1987. Heat of Reaction of Molten Zirconium with UO_2, NUREG/CR-4890. PNL-6165, Pacific Northwest Laboratory, Richland. Washington.

Bunnell, L. R., G. B. Mellinger, J. L. Bates and C. R. Hann. 1977. High-Temperature Properties of Zircaloy-Oxygen Alloys. EPRI NP-524, p. 85.

Bunnell, L. R. and J. T. Prater. 1986. Viscosity of Zr-UO_2 Mixtures at 1800 to 2100°C. NUREG/CR-4495. PNL-5627, Pacific Northwest Laboratory, Richland, Washington.

Cathcart, J. V., and R. E. Pawel. August 1977. Zirconium Metal-Water Oxidation Kinetics: IV. Reaction Rate Studies. ORNL-NUREG-17, Oak Ridge National Laboratory, Oak Ridge, Tennessee.

Chung, H. M., and G. R. Thomas. 1981. The Retarding Effect of Hydrogen on Zircaloy Oxidation. NSAC-29, Nuclear Safety Analysis Center, Argonne, Illinois.

Chung, H. M., and G. R. Thomas. 1983. Zircaloy Oxidation and Hydrogen Generation Rates in Degraded Core Accident Situations. CONF-821026-13.

Hobson, D. O., and P. L. Rittenhouse. January 1972. Embrittlement of Zircaloy-Clad Fuel Rods by Steam During LOCA Transients. ORNL-4758, Oak Ridge National Laboratory, Oak Ridge, Tennessee.

Hofmann, P., and C. Politis. 1979. "The Kinetics of the Uranium Dioxide-Zircaloy Reactions at High Temperatures," J. Nuclear Materials 87 (1979) pp. 375-397.

Hofmann, P., D. Kerwin-Peck, and P. Nikolopoulos. 1984. "Physical and Chemical Phenomena Associated with the Dissolution of Solid UO_2 by Molten Zircaloy-4," Zirconium in the Nuclear Industry, 6th International Symposium, ASTM STP 824, eds. D. G. Franklin and R. B. Adamson, American Society for Testing and Materials. pp. 810-834.

Ikeda, S., G. Ito, and S. Ohashi. 1975. J. Metals of Japan 39:70.

Leistikow, S., G. Schanz, and H. Berg. March 1978. Kinetics and Morphology of Isothermal Steam Oxidation of Zircaloy at 700-1300°C. Kfk-2587, NRC Translation 553.

Levin, E. M., and H. F. McMurdie. 1975. Phase Diagrams for Ceramists - 1975 Supplement. American Ceramic Society, p. 17.

Parker, W. J., R. K. Jenkins, C. P. Butler, and G. L. Abbott. 1961. "Flash Method of Determining Thermal Diffusivity, Heat Capacity and Thermal Conductivity," J. Appl. Phys. 32, no. 9, pp. 1679-1684.

Pawel, R. E. 1979. Oxygen Diffusion in the Oxide and Alpha Phases During Reaction of Zircaloy-4 With Steam From 1000° to 1500°C. J. Electrochem. Soc. Vol. 126, no. 7, pp. 1111-1118.

Prater, J. T., and E. L. Courtright. 1986. High Temperature Oxidation of Zircaloy-4 in Steam and Steam-Hydrogen Environments. NUREG/CR-4476, PNL-5558, Pacific Northwest Laboratory, Richland, Washington.

Prater, J. T., and E. L. Courtright. 1987. Zircaloy-4 Oxidation at 1300 to 2400°C. NUREG/CR-4889. PNL-6166, Pacific Northwest Laboratory, Richland, Washington.

Rasmussen, J. J., et al. 1971. Structure-Property Relationship in Liquid Ceramics. Y-49027, Office of Naval Research, Contract N00014-67-C-0341. NR 032-501.

Ruh, R., and H. J. Garrett. 1967. "Nonstoichiometry of ZrO_2 and Its Relation to Tetragonal-Cubic Inversion in ZrO_2." J. Am. Cer. Soc. 50(5):258.

Sawatzky, A., G. A. Ledoux, and S. Jones. 1977. "Oxidation of Zirconium During a High Temperature Transient." Zirconium in the Nuclear Industry, ASTM STP 633, eds. A. L. Lowe, Jr., and G. W. Parry, pp. 143-149.

Skokan, A. 1984. "High-Temperature Phase Relations in the U-Zr-O System." In Proceedings of the 5th International Meeting on Thermal Nuclear Reactor Safety, Vol. 2, eds. G. Bork and H. Rininsland, pp. 1035-1042. Kernforschungszentrum, GmbH, Karlsruhe, Federal Republic of Germany.

Suzuki, M., S. Kawasaki, and T. Furuta. 1977. Zircaloy Steam Reaction and Embrittlement of the Oxidized Zircaloy Tube Under Postulated Loss of Coolant Accident Conditions (Oxidation Kinetics and Embrittlement of Zircaloy at Above 1200°C). NUREG/TR-0014, U.S. Nuclear Regulatory Commission, Washington, D.C.

Urbanic, V. F., and T. R. Heidrick. 1978. "High-Temperature Oxidation of Zircaloy-2 and Zircaloy-4 in Steam." J. Nucl. Mat. 75:251-261.

U.S. Code of Federal Regulations. 1981. Title 10, Part 50, Appendix K, Paragraph I.5, p. 429.

DISTRIBUTION

No. of Copies

OFFSITE

10 R. Van Houten
U.S. Nuclear Regulatory Commission
Office of Nuclear Regulatory Research
1130-SS
Washington, D. C. 20555

M. P. Manahan
Battelle Columbus Laboratories
505 King Avenue
Columbus, OH 43201

D. Hagrman
EG&G Inc.
Idaho National Engineering Laboratory
P.O. Box 1625
Idaho Falls, ID 83415

W. Mings
EG&G Inc.
Idaho National Engineering Laboratory
P.O. Box 1625
Idaho Falls, ID 83415

C. Allison
EG&G Inc.
Idaho National Engineering Laboratory
P.O. Box 1625
Idaho Falls, ID 83415

FOREIGN

H. Bairiot
Belgonucleaire S. A.
Rue de Champ de Mars 25
B-1050 Brussels
BELGIUM

No. of Copies

J. Basselier
Belgonucleaire S. A.
Rue de Champ de Mars 25
B-1050 Brussels
BELGIUM

P. Fehrenbach
Atomic Energy Canada Ltd.
Chalk River, Ontario
CANADA KOJ 1JO

E. Kohn
Atomic Energy Canada Ltd.
Sheridan Park Research Comm.
Mississauga, Ontario
CANADA L5K 1B2

D. Nishimura
Atomic Energy Canada Ltd.
Chalk River, Ontario
CANADA KOJ 1JO

H. Rosinger
Atomic Energy Canada Ltd.
Pinawa, Manitoba
CANADA ROE 1LO

C. Blahnik
Ontario Hydro
Toronto, Ontario
CANADA M5G 1X6

J. P. Longworth
Central Electric Generating Board
Berkeley Nuclear Labs
Berkeley, Gloucester GL13 9PB
ENGLAND

F. Abbey
UK Atomic Energy Authority
SRD
Culcheth, Warrington WA3 4VE
ENGLAND

No. of Copies

T. Butland
UK Atomic Energy Authority
RX Systems Analysis Div.
Winfrith, Dorchester
Dorsett DT2 8DH
ENGLAND

M. Hayns
UK Atomic Energy Authority
SRD
Culcheth, Warrington WA3 4VE
ENGLAND

R. Potter
UK Atomic Energy Authority
RX Systems Analysis Div.
Winfrith, Dorchester
Dorsett DT2 8DH
ENGLAND

J. Stephenson
UK Atomic Energy Authority
SRD
Culcheth, Warrington WA3 4VE
ENGLAND

A. Fiege
Kernforschungszentrum
Postfach 3640
7500 Karlsruhe
FEDERAL REPUBLIC OF GERMANY

S. Hagen
Kernforschungszentrum
IT-CP
Postfach 3640
7500 Karlsruhe
FEDERAL REPUBLIC OF GERMANY

P. Hofman
Kernforschungszentrum
IMF/1
Postfach 3640
7500 Karlsruhe
FEDERAL REPUBLIC OF GERMANY

No. of Copies

H. Rininsland
Kernforschungszentrum
Postfach 3640
7500 Karlsruhe
FEDERAL REPUBLIC OF GERMANY

W. Schock
Kernforschungszentrum
Aerosol Physics Laboratory
Postfach 3640
7500 Karlsruhe
FEDERAL REPUBLIC OF GERMANY

E. Manilia
Enea Nucl Energ Alt Disp
Via V Brancati 48
00144 Rome
ITALY

G. Petrangeli, Dire R. D. S.
Enea Nucl Energ Alt Disp
Via V Brancati 48
00144 Rome
ITALY

G. Saponaro
Enea Nucl Energ Alt Disp
Via V Brancati 48
00144 Rome
ITALY

K. Hirano
Japan Atomic Energy Res. Inst.
Tokai-Muri Naka-Gun
Ibaraki-Ken 319-11
JAPAN

K. Soda
Japan Atomic Energy Res. Inst.
Tokai-Muri Naki-Gun
Ibaraki-Ken 319-11
JAPAN

No. of
Copies

J. H. Cha
Korea Adv. Energy Research Inst.
Cheung-Ryang
Seoul
SOUTH KOREA

S. K. Chae
Korea Adv. Energy Research Inst.
P.O. Box 7
Daeduk Danji
Chungnam
SOUTH KOREA

H. R. Jun
Korea Adv. Energy Research Inst.
P.O. Box 7
Daeduk Danji
Chungnam
SOUTH KOREA

Y. H. Kang
Korea Adv. Energy Research Inst.
P.O. Box 7
Daeduk Danji
Chungnam
SOUTH KOREA

K. J. Brinkmann
Netherlands Energy Res. Fdtn.
P.O. Box 1
1755ZG Petten NH
NETHERLANDS

M. Bustraan
Netherlands Energy Res. Fdtn.
P.O. Box 1
1755ZG Petten NH
NETHERLANDS

No.of
Copies

Chao-Chin Tung
Atomic Energy Council
67 Lan 144 Sec 4
Keelung Rd.
Taipei, Taiwan
REPUBLIC OF CHINA

Sen-I Chang
Institue of Nuclear Energy Res.
P.O. Box 3
Lungtan
Taiwan 325
REPUBLIC OF CHINA

L. Hammar
Statens Karnkraftinspektion
P.O. Box 27106
S-10252 Stockholm
SWEDEN

K. Johansson
Studsvik Energiteknik AB
S-611 82 Nykoping
SWEDEN

ONSITE

31 Pacific Northwest Laboratory

E. L. Courtright (4)
T. L. Gilbride
P. E. Hart
D. D. Lanning
F. E. Panisko
J. T. Prater (15)
R. E. Williford
Publishing Coordination (2)
Technical Report Files (5)

NRC FORM 335 (2-84) NRCM 1102, 3201, 3202

U.S. NUCLEAR REGULATORY COMMISSION

BIBLIOGRAPHIC DATA SHEET

SEE INSTRUCTIONS ON THE REVERSE

1 REPORT NUMBER (Assigned by TIDC, add Vol. No., if any)

NUREG/CR-4891
PNL-6164

2 TITLE AND SUBTITLE

Properties of Reactor Fuel Rod Materials at High Temperatures
Final Summary Report -- Severe Core Damage Property Tests Program

3 LEAVE BLANK

4 DATE REPORT COMPLETED

MONTH	YEAR
May	1987

5 AUTHOR(S)

J. T. Prater, E. L. Courtright

6 DATE REPORT ISSUED

MONTH	YEAR
July	1987

7 PERFORMING ORGANIZATION NAME AND MAILING ADDRESS (Include Zip Code)

Pacific Northwest Laboratory
P.O. Box 999
Richland, WA 99352

8 PROJECT/TASK/WORK UNIT NUMBER

9 FIN OR GRANT NUMBER

B2455

10 SPONSORING ORGANIZATION NAME AND MAILING ADDRESS (Include Zip Code)

Division of Reactor Accident Analysis
Office of Nuclear Regulatory Research
U.S. Nuclear Regulatory Commission
Washington, DC 20555

11a TYPE OF REPORT

Technical

b PERIOD COVERED (Inclusive dates)

12 SUPPLEMENTARY NOTES

13 ABSTRACT (200 words or less)

This report summarizes work sponsored by the U.S. Nuclear Regulatory Commission Division of Accident Evaluation to investigate those physical properties that are needed to predict the behavior of fuel-rod assemblies during a loss-of-coolant accident. The results include a determination of the oxidation kinetics of Zircaloy and Zircaloy-uranium oxide mixtures in steam and steam-hydrogen gas mixtures at 1300 to 2400°C, viscosity measurements of zirconium-oxide mixtures at 1800 to 2100°C, an estimate of the heat of reaction for the dissolution of uranium oxide by molten zirconium at 2000°C, and thermal diffusivity measurements on prereacted Zircaloy-uranium oxide mixtures at 800 to 1500°C.

14 DOCUMENT ANALYSIS - a KEYWORDS/DESCRIPTORS

High-temperature oxidation
Zircaloy-4
Oxide growth rate

b IDENTIFIERS/OPEN ENDED TERMS

15 AVAILABILITY STATEMENT

Unlimited

16 SECURITY CLASSIFICATION

(This page) Unclassified

(This report) Unclassified

17 NUMBER OF PAGES

18 PRICE

*U.S. GOVERNMENT PRINTING OFFICE: 1987-191-587:60179

UNITED STATES
NUCLEAR REGULATORY COMMISSION
WASHINGTON, D.C. 20555

OFFICIAL BUSINESS
PENALTY FOR PRIVATE USE, $300

SPECIAL FOURTH-CLASS RATE
POSTAGE & FEES PAID
USNRC
WASH. D.C.
PERMIT No. G-67

NUREG/CR-4891

PROPERTIES OF REACTOR FUEL ROD MATERIALS AT HIGH TEMPERATURES

JULY 1987

BEST COPY AVAILABLE